

Prediction of Machining Parameters on Welded Materials using Response Surface Methodology (RSM) and Artificial Neural Network (ANN)

¹Onyiriuka Frank Onyegbulam, ²Achebo Joseph, ³Obahiagbon Kessington, ^{*4}Uwoghiren Frank Omos

Science and Engineering

^{1,2,4}Department of Production Engineering, University of Benin, Benin City, Nigeria.

³Department of Chemical Engineering, University of Benin, Benin City, Nigeria.

E-mail: onyiriukaf@gmail.com, joseph.achebo@uniben.edu, kess.obahiagbon@uniben.edu,

*frank.uwoghiren@uniben.edu

*corresponding author: Uwoghiren Frank Omos

Corresponding author: Uwoghiren F.O.

Accepted: 17/7/2024

Published: 25/7/2024

Abstract In welding processes, achieving the desired weld quality involves a multitude of factors that can interact with each other, thus, impacting key parameters like the cutting force. Some factors hold more significance, while the influence of others is minimal. Determining the optimal combination of these factors to maximize cutting force is a challenging endeavor. This study is focused on the prediction and optimization of machining parameters for welded joints, including depth of cut, cutting speed, and feed rate, in relation to cutting force. To accomplish this, the study utilizes both the Response Surface Methodology (RSM) and Artificial Neural Network (ANN). The central composite design was meticulously created using Design expert software (version 13.0). The RSM analysis produced a coefficient of determination of 0.9961. Additionally, an artificial neural network model was employed to predict output parameters and was compared with the RSM approach. The training of the neural network utilized 70% of the data for training, 15% for validation, and the remaining 15% for testing. The training process extended for a maximum of 1000 epochs, resulting in a coefficient of determination of 0.87834. The study's findings indicate that, in this specific context, the Response Surface Methodology (RSM) outperformed the Artificial Neural Network (ANN) as a predictive model.

Keywords: cutting force, central composite design, response surface methodology, artificial neural network.

Published by GJEST

1. Introduction

The machining sectors are continuously searching for current methods to lessen the forces produced while on metal cutting, increase tool life, and boost surface quality [1]. Deformation of elastic workpieces and the injection of residual subsurface tension when cutting can reduce the precision of machining. It is vital to have a better understanding of how cutting circumstances and tool wear affect finished surfaces and their geometrical flaws so as to forecast the effects of changing cutting forces and surface integrity [2]. Cutting forces play a critical role in machining operations, affecting tool wear, surface quality, and overall machining efficiency. Predicting and optimizing cutting forces is essential to extend tool life and enhance machining processes [3]. Different materials exhibit unique machining characteristics, necessitating specific approaches for predicting and optimizing cutting forces [4]. In real-world

applications, optimizing cutting forces often involves balancing conflicting objectives like minimizing tool wear, enhancing material removal rate, and reducing energy consumption. Multi-objective optimization techniques, including evolutionary algorithms, are used to find Pareto-optimal solutions. Understanding the wear mechanisms that occur during machining is crucial for predicting and optimizing cutting forces. Wear modes include flank wear, crater wear, adhesion, abrasion, and diffusion. Tool material selection significantly impacts tool life and cutting forces [5]. Research in this area explores the development of advanced tool materials like ceramics, carbides, and coatings to enhance tool performance. Techniques to machine learning can be effective tools for machining optimization procedures. The cutting process's machinability and long-term viability can both be improved by longer tool lives. Cutting fluids should ideally be used

to extend tool life. The bulk of cutting fluids, however, are not biodegradable and present serious environmental risks [6]. [7] developed according to the cutting speed (V_c), feed rate (f), and depth of cut (a_p), Regression frameworks based on the Gaussian process are used to estimate 3 factors for cutting, including the cutting force (F_c), surface roughness (R_a), and tool lifespan (T), in fast rotating operations. In the work by [8], the life and cutting force coefficients (CFCs) was established by assessing the machinability performance of additives (phosphate ester (P-ester), mineral oil, and dialkyl pentasulfide). Innovative micro-geometry is crucial to the process of machining. Cutting edges with the proper size and form increase process dependability, tool life, and wear resistance [9]. When cutting materials, tool shape has a big impact on it [10]. [11] created a model to mimic the force of cutting and area to enhance the power skiving process's machining precision and tool life. Internal gear power skiving involves complicated interactions between the workpiece's and tool's relative movement and the efficient rake angle, chip thickness, and direction of cutting. [12] looked into the force of cutting, roughness of the exterior, and tool life to increase the life of the tool and the surface quality that is worked on, which was a pressing issue in the superalloy based on iron twisting. [13] discovered that a rise in force affects the Workpiece-Fixture-Machine-Tool-Cutting Tool (WFMC) system's productivity and longevity of the tool. Recent advancements in machining technology, including high-speed machining, cryogenic machining, and sustainable machining, have led to new challenges and opportunities in predicting and optimizing cutting forces [14]. Predicting and optimizing cutting forces for enhancing tool life and

machining efficiency is a complex and multidisciplinary field of research. It involves a combination of analytical, empirical, and computational methods, as well as an understanding of material properties, tool wear mechanisms, and optimization techniques [15]. Advances in this field contribute to more sustainable and cost-effective machining processes across various industries.

2. Findings and Discussion

In accordance with the findings of this research, amount of input criteria, an experimental design was developed. The matrix was produced using specialized design software. The 2^k factorial design and it made use of the CCD, or central composite design. The 2^k factorial design is for any number of input parameters considered at 2 levels while the CCD is for any input variables deemed to be between levels 3 and 5. Using the design 7.1 program, the central composite design for this investigation was created, it generated 20 runs for the experiment. These test runs included the results of the selected material, along with input and output parameters. Subsequently, Response Surface Methodology (RSM) and an artificial neural network methods were utilized to analyze this matrix. The primary factors taken into account in this paper are cut depth, speed of cutting, feed rate and the results are the cutting force, chip size, chip removal rate and tool life. The free literature that was strategised offered a variety of values for the procedure factors, every factor has two tiers that make up the peak and low.

Table 1: Input variables and their tiers

Factors	Symbol	Coded value	Coded value
		Low (-1)	Peak (+1)
Depth of cut	D	0.009	2.000
Cutting speed	S	149.4	275.5
Feed rate	F	0.001	2.51

Modelling and Optimization utilizing Response Surface Methodology (RSM)

An effort is made in this research to create a second order mathematical relationship between specified input factors, which consist of the rate of feed, cutting depth, and speed coupled with the response variable, namely;

cutting force employing the RSM (response surface methodology). The optimization model's goal was to maximize cutting force.

To check for model suitability, the squares' sequential sum is required, the consecutive square sum for cutting force response as seen in Table 1.

Table 1 Sum of Squares in a Sequential Model cutting force

Origin	Sum of Squares	df	Avg Square	F-value	p-value	
Avg vs Total	2.672E+07	1	2.672E+07			
Linear vs Avg	2724.76	3	908.25	0.4963	0.6900	
2FI vs Linear	17572.37	3	5857.46	6.50	0.0063	
Quadratic vs 2FI	11583.86	3	3861.29	310.88	< 0.0001	Suggested
Cubic vs Quadratic	96.74	4	24.19	5.28	0.0361	Aliased
Residual	27.46	6	4.58			
Total	2.675E+07	20	1.337E+06			

Table 1 illustrates the Sequential Model Sum of Squares cutting force in which selecting the 'Cubic vs Quadratic' model, indicates that the model is not aliased, but rather the 'Quadratic vs 2FI' was suggested.

To further check for the most suitable model for Cutting Force, a lack of fit test was done and a model with the most insignificant improper fit is selected. The improper fit table for the Cutting Force as displayed in Table 2.

Table 2: Lack of Fit Tests for cutting force

Origin	Sum of Squares	df	Avg Square	F-value	p-value	
Linear	29259.61	11	2659.96	638.39	< 0.0001	
2FI	11687.24	8	1460.90	350.62	< 0.0001	
Quadratic	103.37	5	20.67	4.96	0.0517	Suggested
Cubic	6.63	1	6.63	1.59	0.2628	Aliased
Pure Error	20.83	5	4.17			

From Table 2, The improper fit test further suggested the Quadratic Model the p-value being 0.0517. To further check for the model suitability, the model statistics in brief for the Cutting Force was evaluated; the model with the

highest coefficient of determination is preferable. The summarized data for the cutting force model is indicated in Table 3.

Table 3 :Model Summary Statistics cutting force

Origin	Std. Dev.	R ²	Adjusted R ²	Predicted R ²	PRESS	
Linear	42.78	0.0851	-0.0864	-0.5337	49087.82	
2FI	30.01	0.6342	0.4653	0.1157	28303.78	
Quadratic	3.52	0.9961	0.9926	0.9740	830.88	Suggested
Cubic	2.14	0.9991	0.9973	0.9534	1491.42	Aliased

Table 3 describes the Model Cutting force statistics in summary, in which the R² of the Quadratic model was suggested and that of the cubic aliased. The Variance Analysis for the model was estimated to further examine

the relevance of the quadratic model, the variance analysis (ANOVA) was done for Cutting Force. This as seen in table 4.

Table 4: ANOVA for a quadratic model's cutting force

Origin	Sum of Squares	Df	Avg Square	F-value	p-value	
Model	31880.99	9	3542.33	285.20	< 0.0001	relevant
A-depth of cut	3.59	1	3.59	0.2889	0.6027	
B-cutting speed	129.45	1	129.45	10.42	0.0090	
C-feed rate	2591.72	1	2591.72	208.66	< 0.0001	
A B	10.13	1	10.13	0.8152	0.3878	
A C	17391.12	1	17391.12	1400.17	< 0.0001	
B C	171.13	1	171.13	13.78	0.0040	
A ²	2203.37	1	2203.37	177.40	< 0.0001	
B ²	7959.91	1	7959.91	640.86	< 0.0001	
C ²	3404.55	1	3404.55	274.10	< 0.0001	
Residual	124.21	10	12.42			
Lack of Fit	103.37	5	20.67	4.96	0.0517	not relevant
Pure Error	20.83	5	4.17			
Cor Total	32005.20	19				

This algorithm's F-value of 285.20 from Table 4 indicates the algorithm is relevant. An F-value this high could occur because 0.01% of any given moment to noise. When the P-value is less 0.0500, algorithm items are thought to relevant. In this situation, key algorithm items are B, C, A C, B C, A², B², and C². Should the figure surpass 0.1000, algorithm terms are not relevant. If your algorithm is filled with extraneous items (except those needed to uphold order), algorithm reduction could make

it better. The 4.96 Lack of Fit F-value indicates that there exists 5.17% probability that noise could generate a notable F-value for Lack of Fit. We don't want this since we desire the model to fit. It is concerning that this chance is so low (<10%).

To check for the strength of the model developed the goodness of fit statistics test is done based on the cutting force given in Table 5.

Table 5: Goodness of Fit Statistics for Cutting Force

Std Dev	3.52	R²	0.9961
Avg	1155.80	Adjusted R²	0.9926
C.V. %	0.3049	Predicted R²	0.9740
		Adeq Precision	52.1865

From Table 5, varying by less than 0.2, the Predicted R² of 0.9740 also the Modified R² of 0.9926 are reasonably in agreement. With sufficient accuracy, the ratio of signal to noise is recorded. A proportion of at least four is optimal. A 52.187 ratio implies a reliable signal. Use this algorithm to move about the design space.

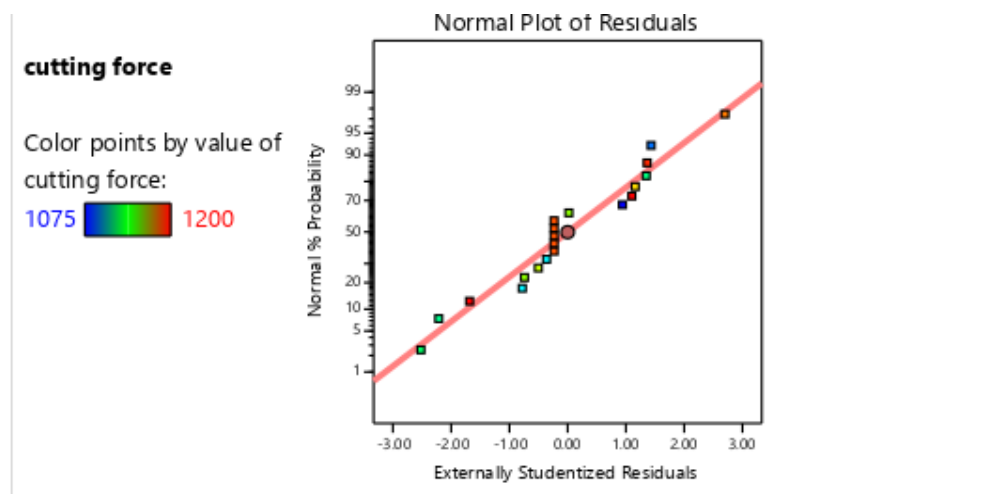
To develop the optimal equation to improve the Cutting Force, the coefficient estimate is determined. The coefficient estimate statistics for Cutting Force is shown in Table 6.

Table 6: Coefficient Estimate Statistics for the Cutting Force

Factor	Coefficient Estimate	df	Standard Error	95% CI Low	95% CI High	VIF
Intercept	1190.79	1	1.44	1187.58	1193.99	
A-depth of cut	0.5126	1	0.9537	-1.61	2.64	1.0000
B-cutting speed	-3.08	1	0.9537	-5.20	-0.9538	1.0000
C-feed rate	-13.78	1	0.9537	-15.90	-11.65	1.0000
AB	1.13	1	1.25	-1.65	3.90	1.0000
AC	-46.62	1	1.25	-49.40	-43.85	1.0000
BC	-4.63	1	1.25	-7.40	-1.85	1.0000
A ²	-12.36	1	0.9284	-14.43	-10.30	1.02
B ²	-23.50	1	0.9284	-25.57	-21.43	1.02
C ²	-15.37	1	0.9284	-17.44	-13.30	1.02

From Table 6, the coefficient estimate illustrates the projected shift in response to each unit shift in the value of the factor when every other factor are held fixed. The average response across every test is the intercept in an orthogonal design. With respect to the factor values, the coefficients change the average nearby. In the case of orthogonal factors, the VIFs are 1. In the case of multi-

colinear components, the VIFs exceed 1. The VIF enhances the degree of the component link's intensity. VIFs under 10 are typically seen as appropriate. To show the model is suitability for the data with respect to Cutting Force, a normal plot of residuals for Cutting Force appears in Fig. 1.

**Figure 1:** Normal Plot of Residuals for Cutting Force

The straight line will run between the locations when the residuals in the chart are of normal probability are dispersed normally. Even a common data set is accompanied with a substantial scatter. The typical residuals cutting force plot revealed a moderate scatter indicating that the data is normal.

To detect for the presence of mega patterns or expanding variance a plot of residuals and the predicted was produced for Cutting Force this as depicted in Figure 2.

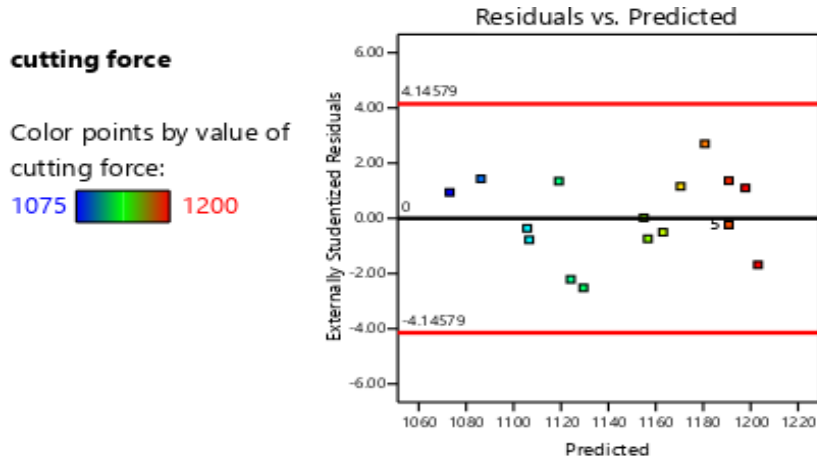


Figure 2: Residual vs. Predicted Cutting Force Plot

For Cutting Force, as Figure 3 illustrates, the anticipated numbers are plotted against the real numbers

for the purpose of detecting a value or collection of values that the model is having difficulties recognizing.

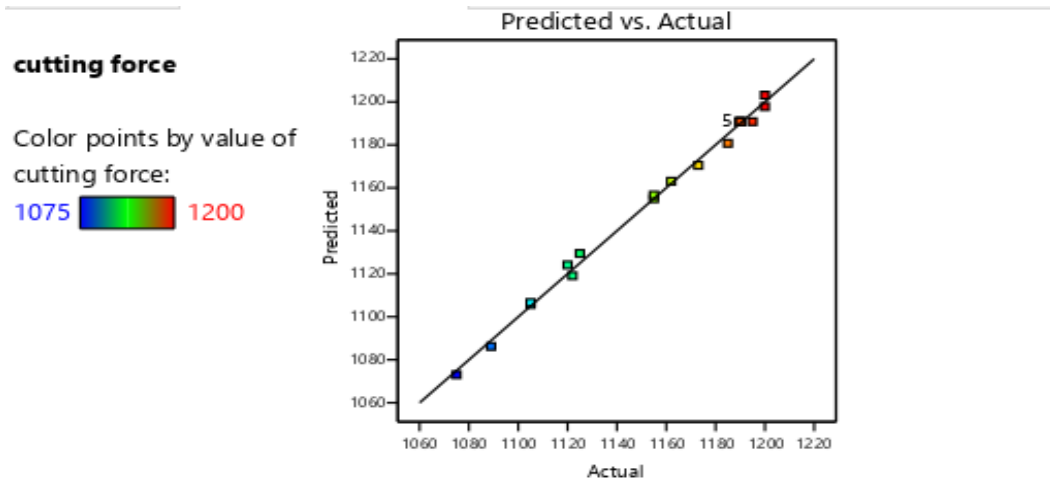


Figure 3: Plot of Predicted Versus Actual for Cutting Force

The dots are roughly near to the line of fit, as shown in Figure 3, indicating that the framework is capable of forecasting the majority of the data dots.

The cook's distance plot for Cutting Force was created to find any possible anomalies in the test results. When an outlier is eliminated from the analysis, the cook's distance is employed to calculate the amount that the regression will change. A spot that sticks out from the rest by having a very high distance value ought to be looked into. The cook's distance which was created for the Cutting Force is shown in Fig. 4.

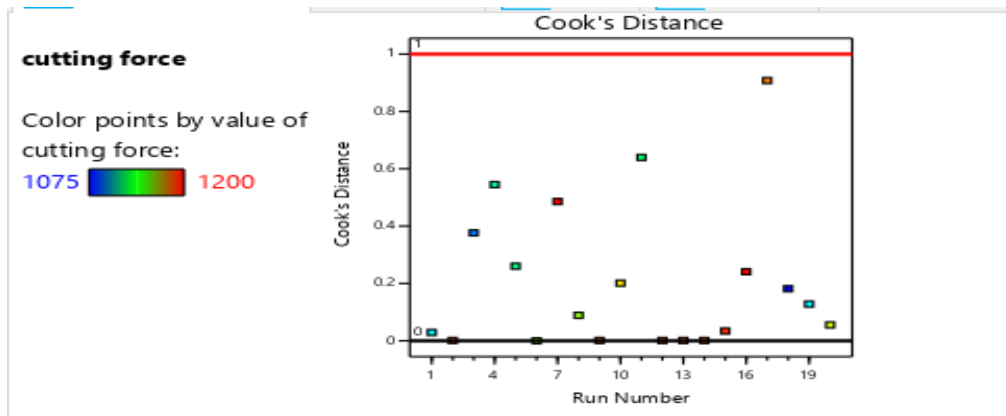


Figure 4: Cook Distance for Cutting Force

The Surface Plot in Figure 5 displays the impact of cutting force, cutting speed, and depth of cut. An increase in the cutting speed and depth of cut yields a corresponding increase in the cutting Force

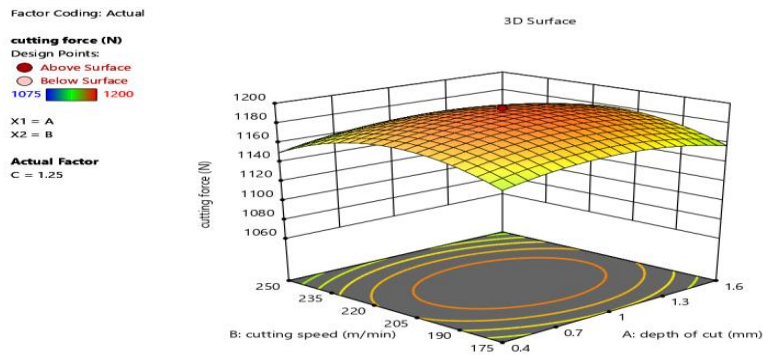


Figure 5 3D plot of cutting depth and speed on cutting force

The 3D Surface Plot in Figure 6 shows the relationship of the feed rate and depth of cut with the cutting force.

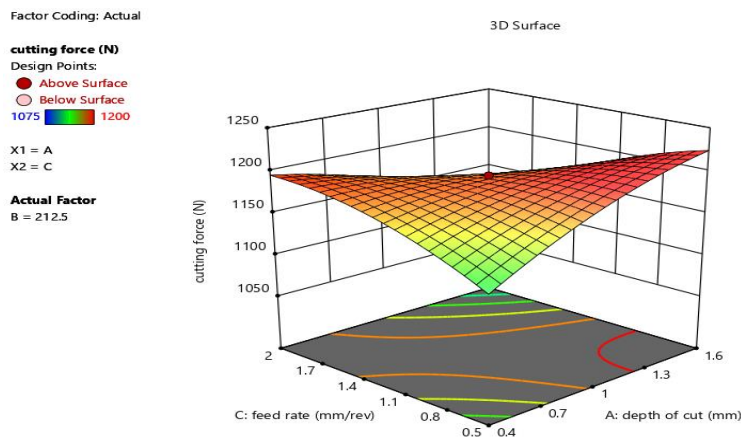


Figure 9 3D plot of Feed rate and cut depth's impact on cutting force

The 3D Surface Plot in Figure 7 illustrates the effect of the feed rate and cutting speed with the cutting force.

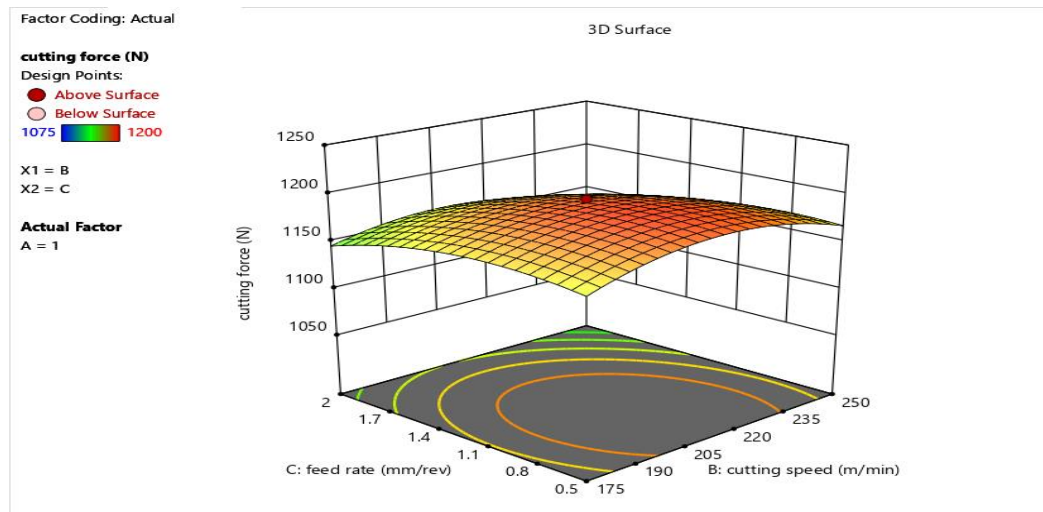


Figure 7: 3D plot Rate of feed and cutting speed's impacts on Cutting Force

The Surface Plot it demonstrates the rate of feed and cutting speed's impacts on Cutting Force reveals that increase in Rate of feed as well as speed of cut result in the increase of the Cutting Force. However, the speed of cut has a stronger influence on the Force of Cutting

Modelling and prediction using Artificial Neural Network (ANN)

Twenty data arrays from experiments, obtained by reproducing the layout matrix from Central Composite Design, was employed for training the neural network model. The process of selecting and training the network structure is crucial for effective data modeling and prediction. Two key factors played a pivotal role in determining the optimal network architecture. Firstly, the choice of the most suitable training algorithm or learning rule was considered. Secondly, the determination of the ideal number of hidden neurons was crucial. To achieve this, a variety of training algorithms and numbers of concealed neurons were selected and evaluated to determine the training algorithm and the optimal count of hidden neurons that would result in the most precise network structure.

However, the selectivity is based on the r^2 and MSE

values. Matlab R2022a is used in the analysis for the Artificial neural network. The Levenberg Marquardt Back Propagation training algorithm, was employed to create the network architecture. In order to generate a network that has been developed employing the Levenberg-Marquardt Back Propagation training technique, different numbers of hidden neurons were chosen. 27 neurons were designated as hidden neurons per layer, and the network's performance was tracked utilizing coefficient of determination (r^2) and MSE. The network generation process divides the input data into three subsets: training data, validation data, and testing data. Specifically, network training required 70% of the data, network validation required 15%, and the remaining 15% was reserved to assess the network's efficiency. The training process continued for a maximum of 1000 epochs. The network was trained using the Trainlm algorithm, which revises the Levenberg-Marquardt optimization-based weight and bias values. Trainlm is known for its efficiency and speed in the toolbox, making it a recommended choice for supervised learning, even though it may require more memory than other algorithms. Figure 8 shows the network diagram created for predicting cutting force using a back propagation neural network, which is based on the Artificial Neural Network architecture 3-27-1.

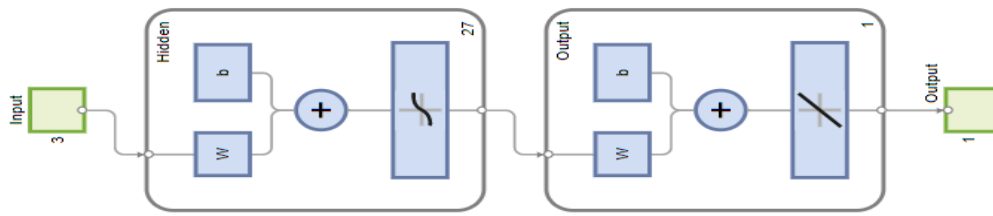


Figure 8: The structure of an artificial neural network

Figure 9 shows the network training chart. From the chart, the network's performance was $1.18e+04$. Validation checks of two (2) was recorded out of six (6).

However, this is to be anticipated given that the raw data's normalization resolved the weight bias issue.

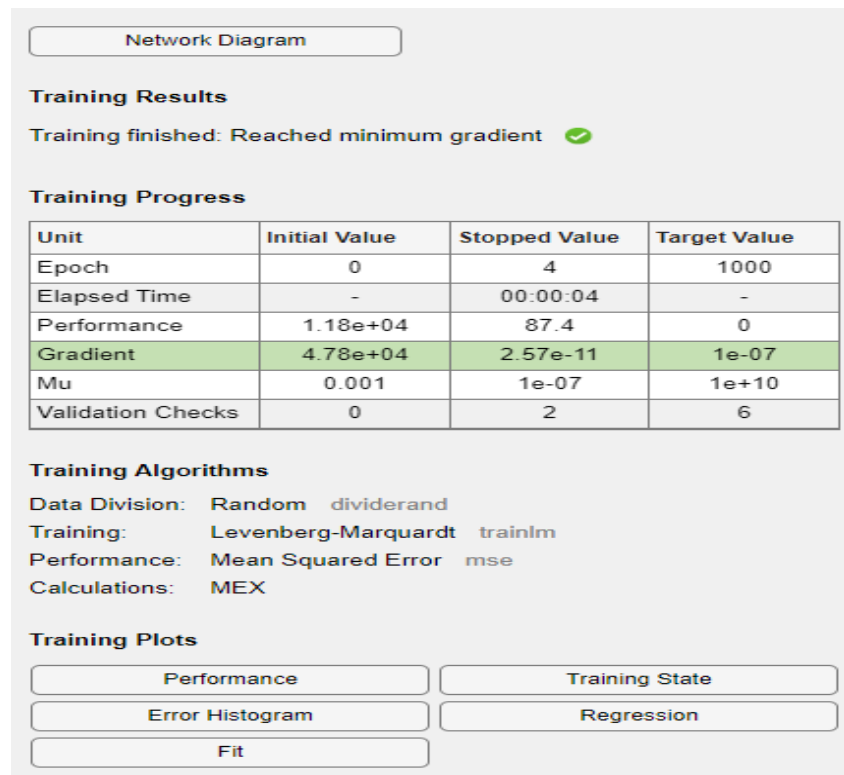


Figure 9: Model Summary for Cutting Force Prediction

Figure 10 displays a graph for performance analysis that illustrates the development of validation, testing, and

training.

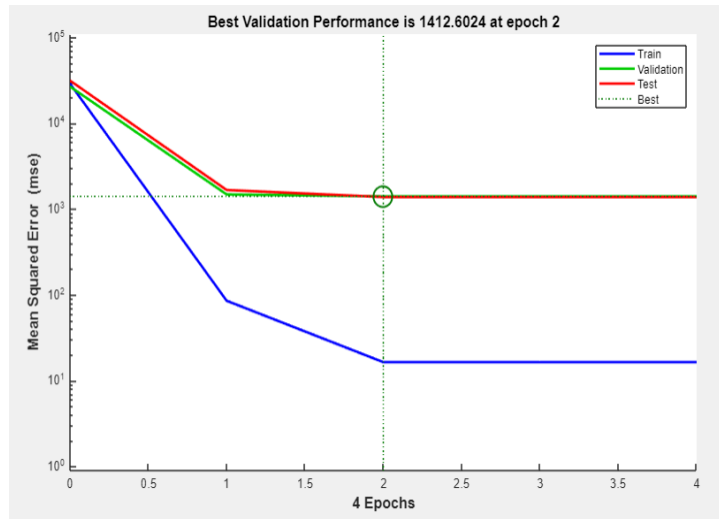


Figure 10 A trained network's performance curve for forecasting of Cutting Force

The performance curve in Fig 15 shows no indication of overfitting. Additionally, a similar tendency was seen in the training, verification, and examination curve's behavior, which was anticipated given that the unprocessed data had already been balanced before usage. A key metric used to assess a network's training

accuracy is lesser mean square error. An error value of 1412.6024 at epoch 2 shows that a network may project the cutting force with an excellent level of precision. Figure 11 displays the training state, which displays the validation check, training gain (μ), and gradient function.

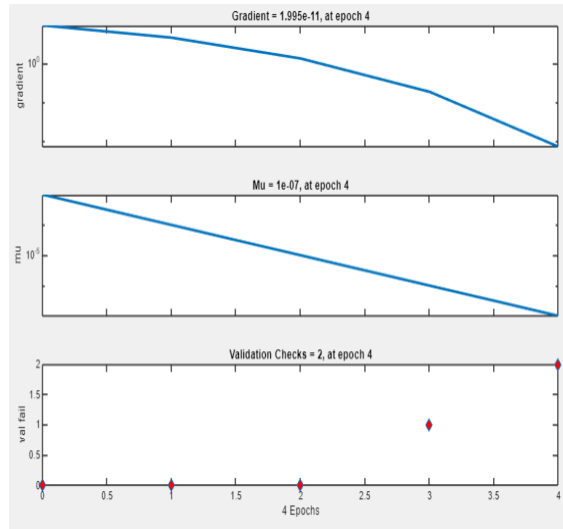


Figure 11: Training State of a Neural Network for Prediction of Cutting Force

Backpropagation is an approach employed in ANN to compute the influence of each neuron's mistake following a batch of data training. In essence, the neural network computes the gradient of the loss function to identify the error generated by the chosen neurons. In this context, lower error values are desirable. A computed gradient

value of $1.995e-11$, as depicted in Figure 11, shows that the erroneous effects of the chosen neurons are exceedingly minimal. Momentum gain (μ) is a crucial controlling variable for the algorithm used in training the neural network. It governs the learning process, and its value must be less than one. A momentum gain of $1e-07$

implies that the network is very capable of forecasting cutting force. The regression plot in Figure 12 illustrates the correlation with relation to the input factors (DOC,

cutting speed, and feed rate) and the target factor (cutting force). It also tracks the progress of learning, verification, and testing during the neural network training process.

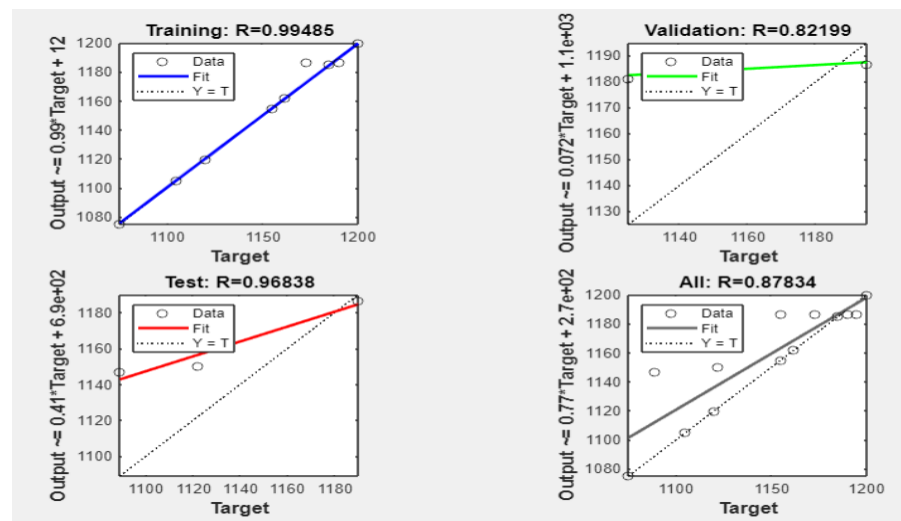


Figure 12: Regression Plot Demonstrating Training, Validation, and Testing Development

It was determined that the network had been correctly trained and could be used to forecast the cutting force based on the computed correlation coefficient (R) values shown in Figure 12.

5. Conclusion

A machined engineering structure's cutting force has an impact on its usable service life. In this research, the development of numerical models using response surface methodology and ANN to enhance and forecast the cutting force, considering cut depth, speed of cutting, and feed rate as input factors. The experimental design adopted was the central design composite, which was generated employing the design 7.1 software the RSM analysis produced optimal solutions with depth of cut of 0.400, cutting speed of 250.000, and rate of feed of 0.500 to produce a machined structure with cutting force of 1106.609, and this was obtained at a desirability value of 0.973. The model of an ANN was also employed to foresee the output parameters and compared with the RSM methodology. From the results obtained the response surface methodology is selected as the better forecasting model over the ANN because it has a higher coefficient of determination.

References

[1] Zhang, Y., & Xu, X. (2021). Machine learning cutting force, surface roughness, and tool life in high speed turning processes. *Manufacturing Letters*, 29, 84-89.

[2] Broderick, M., Turner, S., & Ridgway, K. (2021). Correlation between tool life and cutting force coefficient as the basis for a novel method in accelerated MWF performance assessment. *Procedia CIRP*, 101, 366-369.

[3] Lv, D., Wang, Y., & Yu, X. (2020). Effects of cutting edge radius on cutting force, tool wear, and life in milling of SUS-316L steel. *The International Journal of Advanced Manufacturing Technology*, 111, 2833-2844.

[4] Toubhans, B., Fromentin, G., Viprey, F., Karaouni, H., & Dorlin, T. (2020). Machinability of inconel 718 during turning: Cutting force model considering tool wear, influence on surface integrity. *Journal of Materials Processing Technology*, 285, 116809.

[5] Knápek, T., Dvořáčková, Š., & Váňa, M. (2023). The effect of clearance angle on tool life, cutting forces, surface roughness, and delamination during carbon-fiber-reinforced plastic milling. *Materials*, 16(14), 5002.

[6] Velan, M. V. G., Shree, M. S., & Muthuswamy, P. (2021). Effect of cutting parameters and high-pressure coolant on forces, surface roughness and tool life in turning AISI 1045 steel. *Materials Today: Proceedings*, 43, 482-489.

[7] Onozuka, H., Tayama, F., Huang, Y., & Inui, M. (2020). Cutting force model for power skiving of internal

gear. *Journal of Manufacturing Processes*, 56, 1277-1285.

[8] Zhang, X., Zheng, G., Cheng, X., Li, Y., Li, L., & Liu, H. (2020). 2D fractal analysis of the cutting force and surface profile in turning of iron-based superalloy. *Measurement*, 151, 107125.

[9] Ali, S., Abdallah, S., & Pervaiz, S. (2022). Predicting cutting force and primary shear behavior in micro-textured tools assisted machining of AISI 630: Numerical modeling and taguchi analysis. *Micromachines*, 13(1), 91.

[10] Karpuschewski, B., Kundrák, J., Varga, G., Deszpoth, I., & Borysenko, D. (2018). Determination of specific cutting force components and exponents when applying high feed rates. *Procedia CIRP*, 77, 30-33.

[11] Imani, L., Rahmani Henzaki, A., Hamzeloo, R., & Davoodi, B. (2020). Modeling and optimizing of cutting force and surface roughness in milling process of Inconel 738 using hybrid ANN and GA. *Proceedings of the Institution of Mechanical Engineers, Part B: Journal of Engineering Manufacture*, 234(5), 920-932.

[12] Gupta, M. K., Korkmaz, M. E., Sarıkaya, M., Krolczyk, G. M., Günay, M., & Wojciechowski, S. (2022). Cutting forces and temperature measurements in cryogenic assisted turning of AA2024-T351 alloy: An experimentally validated simulation approach. *Measurement*, 188, 110594.

[13] Xiao, Q., Yang, Z., Zhang, Y., & Zheng, P. (2023). Adaptive optimal process control with actor-critic design for energy-efficient batch machining subject to time-varying tool wear. *Journal of Manufacturing Systems*, 67, 80-96.

[14] Jeyapandiarajan, P., & Xavier, A. (2019). Influence of cutting condition on machinability aspects of Inconel 718. *Journal of Engineering Research*, 7(2).

[15] Kuntoğlu, M., Aslan, A., Pimenov, D.Y., Usca, Ü.A., Salur, E., Gupta, M.K., Mikolajczyk, T., Giasin, K., Kapłonek, W. and Sharma, S., (2020). A review of indirect tool condition monitoring systems and decision-making methods in turning: Critical analysis and trends. *Sensors*, 21(1), p.108.